This paper reports the results of calculating the magnetic parameters for a direct dipole magnet in the system of vertical convergence-separation of particle beams of the upper and lower rings of the heavy-ion collider. An optimized variant of the yoke and superconducting winding structures has been obtained, providing for the assigned value of a homogeneous magnetic field inside the aperture at the minimized contributions of higher-order harmonics, average-integral along the length. The results from the analysis of the transverse projections of the magnetic induction obtained by 2D modeling of two variants of the design of the central cross-section of the dipole electromagnet are presented. The analysis results have established the dependence of the stability of magnetic parameters in the aperture of the electromagnet when the current in the winding changes on the volume of those yoke regions whose magnetization value is close to saturation. A 3D model of the magnetically active part has been built for two variants of the electromagnet design, and the values of the average-integral harmonics of transverse projections of magnetic induction in the aperture have been calculated. The relationship between the third average-integral harmonic of magnetic induction and the size lengths of the yoke and winding has been empirically established, making it possible to correct the heterogeneity of the transverse magnetic field in the aperture of the electromagnet. The results of optimization of the structure of the magnetically active part of the electromagnet are presented on the criteria for a minimum of the values of the average-integral coefficients of magnetic induction, carried out on the basis of correction of the initial geometric parameters of the yoke and winding. An improvement in the stability of magnetic parameters has been demonstrated, by 3 times, as well as a two-fold reduction in the contribution to the heterogeneity by the third average-integral harmonic when using a two-row arrangement of the winding turns inside the yoke in the design of the electromagnet

Keywords: dipole electromagnet, superconducting winding, beam of particles, magnetic field harmonic coefficient

UDC 621.318.372
DOI: 10.15587/1729-4061.2021.228655

DESIGNING A STRUCTURE OF THE MAGNETICALLY ACTIVE PART OF DIPOLE ELECTROMAGNETS FOR THE SYSTEM OF VERTICAL CONVERGENCE-SEPARATION OF BEAMS

Andriy Getman
Doctor of Technical Sciences,
Senior Researcher
Department of Theoretical
Electrical Engineering
National Technical University
«Kharkiv Polytechnic Institute»
Kyrpychova str., 2, Kharkiv, Ukraine, 61002
E-mail: getmanav70@gmail.com

Received date 28.02.2021
Accepted date 01.04.2021
Published date 22.04.2021

How to Cite: *Getman, A. (2021). Designing a structure of the magnetically active part of dipole electromagnets for the system of vertical convergence-separation of beams. Eastern-European Journal of Enterprise Technologies, 2 (5 (110)), 14–22. doi: https://doi.org/10.15587/1729-4061.2021.228655*

1. Introduction

The electromagnets used in the accelerating equipment differ significantly in their structure from those applied in various electrical machines and electronic devices. This is due to the fact that the electromagnets of particle accelerators have a fundamentally different purpose. In cyclical accelerators, electromagnets have two functions: the formation of the size of a beam of particles and ensuring the stability of their movement in orbit. The practical solution to these two tasks relates to the creation of the predefined spatial distribution of the magnetic field in the aperture of the electromagnet – the volume of a vacuum chamber with moving charged particles. At the same time, there are quite high requirements for the accuracy of creating a magnetic field in the aperture of the electromagnet. In practice, the relative deviation from the predefined spatial distribution of the magnetic field is limited to a value of about 10^{-4}.

An additional complicating requirement is the creation of the maximum possible magnetic induction by electromagnets as its increase reduces the size of the accelerator's orbit. To minimize the consumption of electricity in accelerators with particle energy up to 500 GeV, the structure of electromagnets includes a magnetic core of ferromagnetic material. However, the phenomenon of magnetic saturation of the yoke material leads to a limit of up to 2 T of the maximum value of magnetic induction created by the electromagnet. Therefore, in accelerators designed for large particle energy values, magnetic induction of about 10 T is induced by superconducting windings located inside the ferromagnetic screen.

For accelerators with particle energy of about 10 GeV (SIS 100, NICA) it is economically justified to create compact electromagnets, in the design of which superconducting current windings are used together with the ferromagnetic bright. Therefore, it is additionally necessary to take into consideration the changes in the design and magnetic properties of the electromagnet material when cooled to ultra-low (helium) temperatures.

In modern accelerator complexes such as the collider, the function of convergence-separation of two parallel colliding beams to the point of interaction is executed by special dipole electromagnets, which have increased aperture sizes. Increased aperture and the difference between the trajectory of beams from the longitudinal axis of the symmetry of dipole electromagnets for convergence-separation lead to the stricter requirements for the accuracy of ensuring the spatial distribution of the magnetic field being created.

Therefore, it is of practical interest to advance methods for developing the structure of the magnetically active part of the dipole electromagnets with a superconducting current winding that could provide for the creation of a magnetic field in the aperture with the accuracy specified by specification.

2. Literature review and problem statement

Underlying the simplest model of beam dynamics in the magnetic field of accelerators electromagnets is disregarding the cross-sectional components of particle speed. This assumption makes it easier to describe the force impact of a transverse magnetic field on particles that move longitudinally in the accelerator orbit [1]. In this model, the homogeneous component of the magnetic field of the dipole electromagnet is described as the «main field», and all the unevenness of its spatial distribution is set by circular harmonics higher than the dipole, taken with some weights. Thus, the task of ensuring the specified force effect of the magnetic field on the beam of particles is reduced to the creation of the desired value of the «main field» at the minimized weight ratios of higher harmonics.

However, the application of the circular harmonics model is mathematically correct only for the central cross-section of the electromagnet, where the magnetic field can be considered flat parallel (a 2D distribution). The real distribution of the magnetic field in the electromagnet aperture is 3D, which is especially pronounced on its ends. Therefore, in practice, such harmonics are used that are termed average-integral lengthwise the electromagnet, introduced as the averaged values of the harmonics calculated in the planes of the cross-section of the aperture [2]. At the same time, the average-integral harmonic coefficients must be calculated based on the values of magnetic induction derived from a numerical or physical experiment. Thus, the shortcomings of the model's theoretical base are compensated for by enlarging the experimental part of the research.

On the other hand, the analytically precise construction of 3D mathematical models based on the Bio-Savard law is known only for current winding without the iron core of the electromagnet [3]. Similarly, the use of a current winding model based on the spherical harmonics of the magnetic field does not resolve the problem of synthesizing the entire magnetic part of the electromagnet [4].

Models that use special control functions for parametric beam control [5] are focused on calculating the dynamic characteristics of the beam in the accelerator. In such models, magnetic field data are used as a baseline for subsequent calculation, which does not make it easier to create and optimize the structure of electromagnets.

Another direction to improve the model of average-integral harmonics of the magnetic field of electromagnets is to use, to describe the field in the aperture with an elliptical cross-section, elliptical harmonics instead of circular ones [6]. However, such an advancement of the model does not rule out the need to conduct experimental studies into the longitudinal distribution of the magnetic field in the electromagnet aperture.

There is also a way to improve the spatial distribution of the magnetic field in the aperture by small ferromagnetic overlays (shims) inside the electromagnet's core [7]. However, in the case of a wide range of particle energies used in accelerator experiments, such as the NICA collider [8], this approach is ineffective since the non-linear nature of magnetization of ferromagnetic overlays when the current in the superconducting current winding deviates from some optimal value would lead to a deterioration in the homogeneity of the magnetic field.

At the maximum values of the magnetic induction created by the electromagnet, the dependence of magnetization of its ferromagnetic yoke demonstrates a pronounced non-linear character on the current in the winding. That, in turn, leads to a deterioration in the homogeneity of the magnetic field created in the aperture at current values different from the rated ones. To level off this negative factor, the practical range of working currents in superconducting windings is limited [9]. When calculating the basic parameters for an electromagnet structure, the rated current value in the winding is used.

One of the ways described in [10] to reduce the volume of physical modeling in the development of electromagnets with a superconducting current winding is the algorithm of applying analytical and numerical calculations of the magnetic field in the aperture. Underlying this approach are the empirically established ratios that make it possible to change the values of average-integral harmonics by a slight correction of the geometry of a current winding. However, the algorithm and ratios described in the method were devised relative to the design of quadrupole electromagnets. However, there is an obvious practical interest in finding similar dependences that make it easier to design and optimize the structure of dipole electromagnets. A particular application of this method can be practical recommendations for the construction of a magnetically active part of the dipole electromagnets in the collider colliding beams convergence-separation system.

3. The aim and objectives of the study

The aim of this work is to optimize the structure of the magnetic field in the aperture of the dipole electromagnet in the system of vertical convergence-separation of beams by finding a variant of the structure of the magnetic part with a specified value of homogeneous magnetic induction and minimized contributions by the average-integral coefficients of higher-order harmonics. This would ensure the convergence-separation of two oncoming moving beams of particles of the upper and lower ring of the collider at the point of heir interaction.

To accomplish the aim, the following tasks have been set:

– to choose the optimal structure of the central cross-section and calculate the magnetic characteristics of a 2D model of the magnetic field of the BV1 type dipole magnet for the system of vertical convergence-separation of collider beams of the NICA accelerating complex;

– to build for the basic version of the structure of the BV1 electromagnet a 3D magnetic field model in the aperture and to calculate the average-integral magnetic induction coefficients;

– to construct an empirical expression for calculating the third average-integral harmonic of magnetic induction based on the correction of the geometric parameters of the BV1 electromagnet yoke and winding, and to optimize the magnetic parameters of the two variants of the BV1 electromagnet structure according to the criterion for a minimum of the average-integral values of the third and fifth harmonics of the magnetic field.

4. Materials and methods to study magnetic field in the aperture of dipole electromagnets

The Joint Institute for Nuclear Research (JINR) plans to build a collider of heavy ions [11]. Collisions of beams of particles from two vertically dispersed, parallel rings are organized at two points of the collider perimeter. The function of beam convergence from two rings to the point of interaction and subsequent separation of particles in a vertical direction is performed by the system of vertical convergence-separation. The system consists of 8 (four for each point of interaction) dipole electromagnets of 2 types, BV1 and BV2. The BV2's magnetically active part is two paired electromagnets with two apertures for the beams of particles of the upper and lower rings of the collider. The BV1 electromagnet has a «common» vacuum chamber for both beams of particles. Due to the oncoming direction of movement of the two beams inside the BV1 aperture, its magnetic field deflects the trajectories of particles opposite vertically.

For convenience, this work considers, instead of the vertically-deviating BV1 electromagnet, a horizontally-turning electromagnet. The vertical axis of the actual magnet should correspond to the horizontal axis in the work, and horizontal – to vertical.

This work explores the relationship between the spatial structure of the magnetic field and the parameters of the structure of the magnetic part of the BV1 dipole electromagnet with a superconducting current winding, whose general view is shown in Fig. 1.

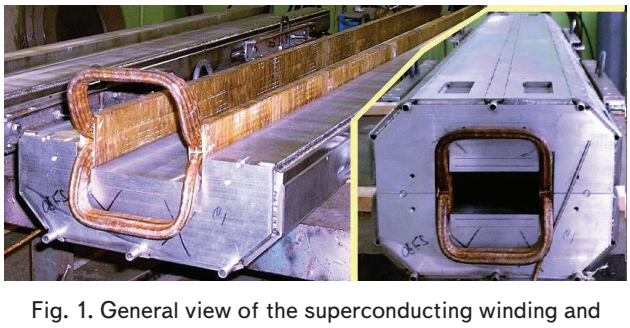

Fig. 1. General view of the superconducting winding and magnetically active part of the dipole electromagnet

Therefore, of the entire set of subsystems and devices in the direct dipole electromagnet, only its magnetically active part is considered that creates a magnetic field. Components of the magnetically active part are: a superconducting winding and a steel yoke (Fig. 2, 3) are represented in this work in a simplified form without elements of cooling, bandage, and attachment, which do not affect the magnetic field of the electromagnet. The parameters given in Table 1 were accepted as the original parameters for designing the structure of the magnetically active part of the BV1 dipole electromagnet.

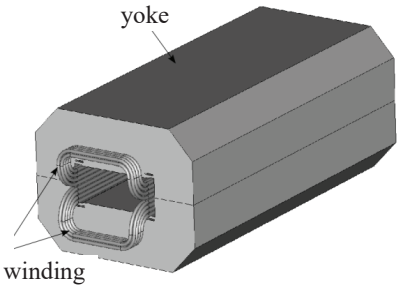

Fig. 2. Simplified view of dipole electromagnet

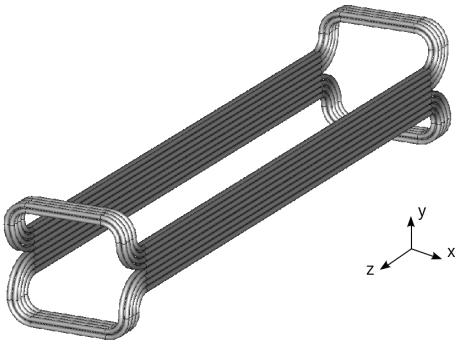

Fig. 3. Simplified view of a superconducting electromagnet winding

Table 1

Initial data to calculate values of the BV1 electromagnet characteristics

Parameter	Value
Overall dimensions of the vacuum chamber [x; y], m	[0.202; 0.162]
Maximum working magnetic field, (T)	1.3
Maximum operating supply current, (kA)	10.4
Rated operational supply current, (kA)	8.25
The number of turns of the superconducting winding	16
Effective length of electromagnet, L_{eff} (m)	1.37
Winding wire outer diameter, (mm)	9.5
Yoke length, L_{yoke} (mm)	1,320
Overall length of the electromagnet, L (mm)	1,471.5
The minimum distance between the center lines of the winding turns, (mm)	10
The minimum bending radius of the winding turns at the end of the electromagnet, (mm)	28.75

Average-integral harmonics are used as the basic characteristics describing the two projections of the magnetic field directed traverse to the movement of the beam in the aperture. The theoretical basis for calculating the values of average-integral harmonics is the representation of the magnetic field in the transverse planes of the aperture set by the applicate z, in the form of a series containing only two cross-sectional projections of the magnetic induction B_ρ and B_φ according to [12]:

$$B_\varphi(\rho,\varphi,z)+iB_\rho(\rho,\varphi,z)= \\ =B_0(z)\sum_{n=1}^{\infty}\left[b_n(z)+ia_n(z)\right]\frac{(\rho)^{n-1}}{R_{ref}^{n-1}}e^{in\varphi}, \quad (1)$$

where ρ, φ, z are the cylindrical coordinates of the magnetic field observation point; $B_0(z)$ is the value of magnetic induction of the «main field»; $b_n(z)$, $a_n(z)$ are the normal and skew magnetic induction coefficients of power n.

In calculating the harmonics of the BV1 electromagnet, the value of the reference radius of the R_{ref} circumference, according to the magnetic induction data on which the $b_n(z)$ coefficients were determined, was chosen equal to 0.07 m.

According to the definition in [12], the average-integral harmonics of magnetic induction in (1) are calculated from the following representation:

$$b_n^* = \frac{\int_{-\infty}^{\infty} b_n(z)B_0(z)\mathrm{d}z}{\int_{-\infty}^{\infty} B_0(z)\mathrm{d}z} = \frac{\int_{-\infty}^{\infty} b_n(z)B_0(z)\mathrm{d}z}{B_c L_{eff}}, \quad (2)$$

$$a_n^* = \frac{\int_{-\infty}^{\infty} a_n(z)B_0(z)\mathrm{d}z}{\int_{-\infty}^{\infty} B_0(z)\mathrm{d}z} = \frac{\int_{-\infty}^{\infty} a_n(z)B_0(z)\mathrm{d}z}{B_c L_{eff}}, \quad (3)$$

where B_c is the magnetic induction value of the «main field» in the central cross-section of the electromagnet; L_{eff} is an effective length of the electromagnet calculated as:

$$L_{eff} = \frac{\int_{-\infty}^{\infty} B_0(z)\mathrm{d}z}{B_c}. \quad (4)$$

Taking into consideration the above assumptions, this work considers a normally oriented dipole electromagnet. Therefore, only normal $b_n(z)$ coefficients from a series (1) are used to describe the magnetic field aperture. The coordinate system is tied to the center of the symmetrical structure of the magnetically active part of the electromagnet, whose longitudinal axis is directed along the applicate axis. The assumption of the electromagnet's axial symmetry has made it possible to reduce the number of terms in a series (1) by excluding the terms with even n.

5. Results of studying the magnetic field parameters of the superconducting winding and the yoke of the BV1 electromagnet

5. 1. Finding the optimal parameters of the central section of the magnetically active part of the BV1 electromagnet (2D calculation)

The structure of the central cross-section of the dipole electromagnet for the vertical convergence-separation of beams of the «window frame» type is based on the tested technological solutions for its fabrication at the factory of electromagnets at JINR. The electromagnet iron yoke is made of silicon steel, mark 2212 (Si-1.3 %). To calculate the magnetic field in the central cross-section of BV1, I used the parameters given in Table 1. Taking into consideration the additional restrictions on the dimensions of BV1, a design option with the winding turns evenly laid for height was initially chosen. The geometry of the central cross-section of the primary structure is shown in Fig. 4 where the dotted line shows the location of the vacuum chamber whose cross-section is elliptical.

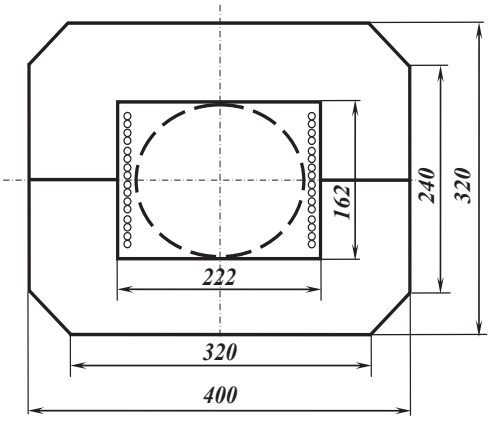

Fig. 4. Dimensions of the central cross-section of the BV1 electromagnet

To improve the homogeneity of the magnetic field inside the aperture of the magnet with the yoke of the «window frame» type, the winding, evenly laid in the window, is pushed in different directions from the center at a short distance [12].

Based on the numerical 2D model of the electromagnet built in the COMSOL4.3 software package, the magnetic field in the central cross-section was calculated. Based on the data obtained thus on the two projections of magnetic induction, on the reference radius, according to [12], a Fourier analysis was performed to calculate values for the circular harmonics' coefficients in (1). As a result of several numerical calculations of the magnetic field and the subsequent assessment of its homogeneity, the optimal position of winding turns was searched for the criterion of a minimum of the third and fifth spatial harmonics of the magnetic field. Thus, it was found that the value of the additional offset from the center of the two identical groups of eight evenly laid turns is 0.5 mm. The found variant of the position of current winding turns (Fig. 5), optimized for the current of the power of superconducting winding of 8.25 kA, was accepted in this work as a baseline.

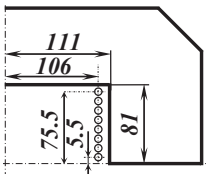

Fig. 5. The fourth part of the central cross-section of the electromagnet for the basic design variant

For the found optimal variant of the position of the turns in the cross-section of the superconducting magnet for the convergence-separation of beams, I calculated the coefficients of circular harmonics at the current values in the winding, which differ from the rated ones, which are given in Table 2.

Table 2

Magnetic field parameters for the variant optimized at 8.25 kA

Winding current	B_0, T	b_3	b_5	b_7
10.4 kA	1.2863692	$2.49911\cdot10^{-4}$	$-0.856\cdot10^{-4}$	$-1.38191\cdot10^{-4}$
8.25 kA	1.0225985	$0.45057\cdot10^{-4}$	$-1.61842\cdot10^{-4}$	$-1.41587\cdot10^{-4}$
6 kA	0.7440359	$0.02263\cdot10^{-4}$	$-1.7965\cdot10^{-4}$	$-1.4185\cdot10^{-4}$
4 kA	0.4960659	$0.02132\cdot10^{-4}$	$-1.8716\cdot10^{-4}$	$-1.41559\cdot10^{-4}$

The analysis of the distribution of magnetic induction inside the aperture of the magnet for the convergence-separation of beams regarding the variant of winding design, optimized at the power current of 8.25 kA has revealed a deterioration in the homogeneity of the magnetic field at the currents of power that differ from the current of the search for an optimum. Therefore, the search was conducted for the structure of the winding optimized for 10.4 kA – the maximum working current of the electromagnet. Based on the previous variant of the structure (Fig. 5), to improve the homogeneity of the field at the current of 10.4 kA, the positions of a pair of extreme winding turns were changed, according to the methodology given in [4]. Next, the above-described calculation of harmonics coefficients (Table 3) was performed; the result of the search for a new variant of the winding design, the positions of the turns were found that are shown in Fig. 6.

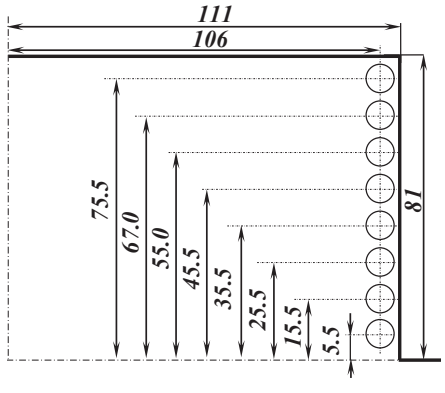

Fig. 6. The fourth part of the central cross-section of the electromagnet (an optimum for the value of winding current of 10.4 kA)

Table 3

Magnetic field parameters for the variant optimized at 10.4 kA

Winding current	B_0, T	b_3	b_5	b_7
10,4 kA	1.2861536	$0.49509\cdot10^{-4}$	$-0.95756\cdot10^{-4}$	$-0.97265\cdot10^{-4}$
8,25 kA	1.0224882	$-1.6725\cdot10^{-4}$	$-1.75503\cdot10^{-4}$	$-1.0091\cdot10^{-4}$
6 kA	0.7439609	$-2.07841\cdot10^{-4}$	$-1.9374\cdot10^{-4}$	$-1.0121\cdot10^{-4}$
4 kA	0.4960167	$-2.08154\cdot10^{-4}$	$-2.01344\cdot10^{-4}$	$-1.0093\cdot10^{-4}$

Thus, two improved variants, for the power currents of 8.25 kA and 10.4 kA, respectively, were found for the position of winding turns in the central cross-section of the yoke of the «window frame» type. The criteria of homogeneity of the magnetic field were the minima of the third and fifth spatial harmonics in the central cross-section. Both variants of the design are characterized by a significant dependence of the coefficients of the third and fifth circular harmonics of the magnetic field on the value of the power current of the electromagnet. The difference between the coefficients taken at the reference radius R_{ref}=0.07 m, at power currents of 10.4 kA and 6 kA, was 2.5×10^{-4} for the coefficients of the third harmonic, and 1.0×10^{-4} for the coefficients of the fifth harmonic. Taking into consideration the standard homogeneity requirement [12] at the level of 1.0×10^{-4}, an alternative design variant was sought. One possible direction of research is a variation of the inner cross-section of the magnetically active part taking into consideration the shape of a vacuum chamber. However, constructing electromagnets with an elliptical cross-section of the yoke and winding is not possible for the existing technology of their development at JINR. Therefore, an intermediate variant with the laying of winding turns in two rows was analyzed, with the addition of rectangular shims in the corners of the yoke. A variant of the structure of such a two-row winding and yoke with shims, shown in Fig. 7, was found on the basis of the criterion for a minimum of the third and fifth spatial harmonics of the magnetic field at a rated power current of 8.25 kA.

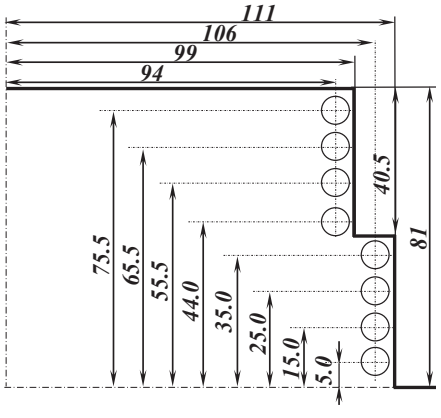

Fig. 7. The fourth part of the central cross-section of the two-row current winding and yoke with shims

For other values of current in a two-row winding, I also calculated coefficients of the harmonics of the magnetic field (Table 4) on the centrally located circumference of R_{ref}=0.07 m. Comparing the calculated parameters of the magnetic field for a standard structure of the «window frame» type and the structure having a two-row winding reveals the following. The two-row variant of the two-row winding structure is characterized by a reduced deviation of the values of the third, fifth, and seventh spatial harmonics of the magnetic field when the power currents of the winding change from 4 kA to 10.4 kA.

Table 4

Magnetic field parameters for the variant of a two-row winding structure optimized at 8.25 kA

Winding current	B_0, T	b_3	b_5	b_7
10,4 kA	1.2882997	$0.64355\cdot10^{-4}$	$-2.76603\cdot10^{-4}$	$-1.84305\cdot10^{-4}$
8,25 kA	1.0229627	$0.64315\cdot10^{-4}$	$-2.65307\cdot10^{-4}$	$-1.77531\cdot10^{-4}$
6 kA	0.7441665	$0.64865\cdot10^{-4}$	$-2.65327\cdot10^{-4}$	$-1.75237\cdot10^{-4}$
4 kA	0.4961299	$0.74122\cdot10^{-4}$	$-2.69154\cdot10^{-4}$	$-1.74326\cdot10^{-4}$

This improvement in the stability of the magnetic field parameters is due to the reduced volume of regions whose magnetization value is close to saturation. This is confirmed by the analysis of the distribution of the magnetization module in the central cross-section of the yoke, derived for the two variants of the electromagnet structure using the 2D model calculations. In Fig. 8, the dotted line marks the regions with the magnetization value close to the saturation of the yoke material. Color scales for magnetization in the fourth part of the central section of the yoke in Fig. 8, *a*, *b* are the same.

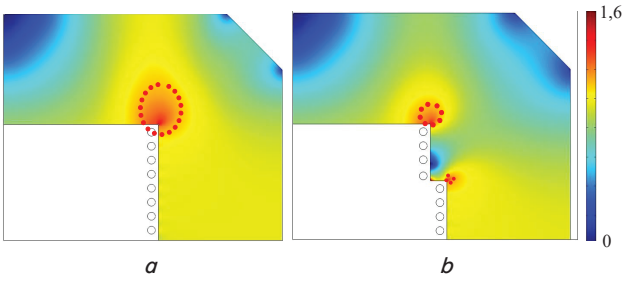

Fig. 8. Distribution of magnetization (×10^6, A/m) in the central cross-section of the yoke: *a* — a variant of the «window frame» structure; *b* — a variant of the structure with a two-row winding

The found variant of the structure with a two-row winding was hereafter considered as an «alternative» compared to the above-described baseline variant.

5. 2. Calculating the magnetic field parameters for a 3D model of the basic variant of the structure of a superconducting winding and a yoke of the BV1 electromagnet

The resulting two variants of the structure of the central cross-section of the electromagnet formed the basis for constructing a 3D model of the BV1 electromagnet.

In addition, to build a 3D model and perform calculations, I used the set parameters for the structure of a superconducting electromagnet for the convergence-separation of beams, given in Table 1.

At the same time, it was noticed that in the case of laying the elements of the winding in one layer, transverse to the longitudinal axis of the electromagnet, the length of BV1 significantly increases. In addition, to reduce the heterogeneity of the magnetic field on the ends of the electromagnet, the transverse elements of winding turns should be removed from the ferromagnetic yoke. Therefore, an attractive option in this regard, enabling the reduction in the excessive elongation of end (protruding beyond the yoke) parts of the current winding, is to arrange the transverse sections of winding turns not in one but in two layers.

The result is the structure of the end part of the winding and the yoke of the electromagnet for the basic variant of the central cross-section of the «window frame» type, whose end view is shown in Fig. 9.

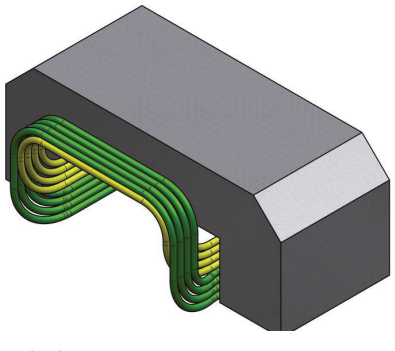

Fig. 9. General view of half of the end side of the electromagnet

Based on the constructed symmetrical 3D model of the electromagnet at the value of the current in the winding of 8.25 kA, the COMSOL4.3 software package was employed for the numerical calculation of two projections of magnetic induction in transverse plane 121, starting from the center with an increment of 10 mm. Based on the 3D calculation of magnetic induction in the aperture on the circles of R_{ref}=0.07 m, a Fourier analysis has helped derive the magnetic field harmonics coefficients from (1) for each of the planes under consideration. The shape of the derived «main field» dependence on the longitudinal coordinate is shown in Fig. 10.

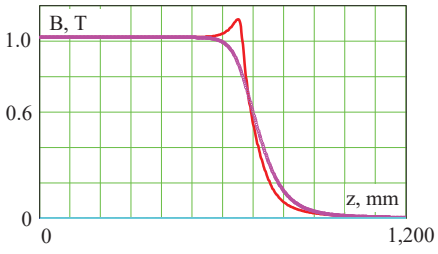

Fig. 10. The dependences of absolute values of the «main field» on the distance between a cross-section to the central section of the magnet (red line) and magnetic induction on the central axis of the magnet (magenta line)

Taking into consideration the symmetry of the electromagnet model, based on the calculation of values of the homogeneous component of magnetic induction, the effective length L_{eff} was calculated from the following formula:

$$L_{eff} = \frac{2}{B_c}\int_0^{1,2} B_0(z)\mathrm{d}z = 1.45112\ (\mathrm{m}). \qquad (5)$$

Using the derived harmonics values in cross-section 121, the values of the average-integral coefficients were also calculated for the third (Fig. 11), fifth, and seventh harmonics of the two magnetic induction projections.

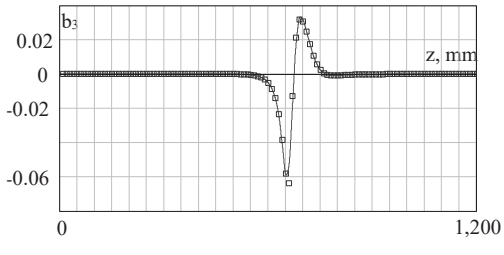

Fig. 11. Dependence of the third harmonic on a longitudinal coordinate

The calculation of the average-integral coefficient of the third harmonic of magnetic induction at a radius of 70 mm was carried out according to the following formula:

$$b_3^* = \frac{2\int_0^{1.2} b_3(z)B_0(z)\mathrm{d}z}{B_c L_{eff}} = -12.2725\cdot 10^{-4}. \qquad (6)$$

Similarly, the average-integral coefficient of the fifth harmonic was calculated according to the following formula:

$$b_5^* = \frac{\int_0^{1.2} b_5(z)B_0(z)\mathrm{d}z}{B_c L_{eff}} = 2.5176\cdot 10^{-4}. \qquad (7)$$

The shape of dependence of the fifth harmonic on the longitudinal coordinate is shown in Fig. 12.

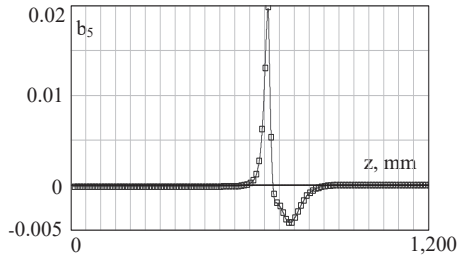

Fig. 12. Dependence of the fifth harmonic coefficient value on the distance of the examined plane to the central section

The functional dependence of the seventh harmonic on a longitudinal coordinate is characterized by the jump-like changes in values near the ends of the electromagnet (Fig. 13).

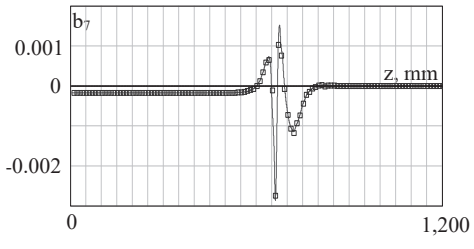

Fig. 13. The dependence of the seventh harmonic coefficient on the distance of the considered magnetic field plane to the center of the electromagnet

The calculation of the average-integral value of the seventh harmonic was carried out according to the following formula:

$$b_7^* = \frac{\int_0^{1.2} b_7(z)B_0(z)\mathrm{d}z}{B_c L_{eff}} = -2.8628\cdot 10^{-4}. \quad (8)$$

The calculation results were obtained for the rated power current value (8.25 kA) of the superconducting winding of the BV1 convergence-separation electromagnet.

5. 3. Results of the optimization of 3D parameters of the magnetic field in a superconducting winding and a yoke of the BV1 electromagnet

The value of the product of the magnetic induction of the «main field» in the central cross-section of the electromagnet B_c by the effective length L_{eff}, obtained as a result of calculating the 3D model, differs from that specified in Table 1. To correct it (in this case, to reduce it), one can successfully apply a change in the entire length of the electromagnet. It should be taken into consideration, in this case, that the contributions to magnetic induction by the yoke and superconducting current winding correlate at about 1:2. Therefore, when calculating a change in the effective length ΔL_{eff} of the electromagnet, considering the relationship of the change in the length of the winding ΔL and the yoke ΔL_{yoke}, the following expression holds in the first approximation:

$$\Delta L_{eff} \approx \frac{2}{3}\Delta L + \frac{1}{3}\Delta L_{yoke}. \quad (9)$$

The above values for the fifth and seventh average-integral characteristics of the homogeneity of the magnetic field in the aperture are close to 10^{-4}. However, the value of the average-integral coefficient of the third harmonic in (6) significantly exceeds the standard values for dipole electromagnets. In order to correct the average-integral coefficient b_3^*, the linear dependence of its magnitude on the difference between the length of the winding and the length of the yoke was empirically established in this work:

$$b_3^* \approx k\left(L - L_{yoke}\right) + p, \quad (10)$$

where k and p are the empirically defined coefficients, for example, by calculating the average-integral coefficient b_3^* for two identical variants of the electromagnet structure with a slight (about 3 mm) difference between winding length and the length of the yoke.

At the same time, my calculations showed a weak correlation of the values of the remaining average-integral coefficients to the difference in the size length of the winding and yoke.

Changing the difference between the length of the yoke and winding based on the described approach, by using (10), has made it possible to reduce the value of the third average-integral harmonic. At the same time, applying (9) to change the effective length has enabled adjusting the dimensions of the magnetically active part of the base model of the electromagnet.

Taking into consideration the relevance of the stability of magnetic characteristics when changing the current of a winding, similar studies were conducted on the alternative structural variant with the laying of longitudinal winding elements in two rows at dimensions corresponding to the basic variant.

The results of the 3D calculation of average-integral harmonics and harmonic coefficients in the central cross-section (at $z=0$), conducted for two values, 8.25 kA and 10.4 kA, of current in the winding, are given in Table 5 (for brevity, the total multiplier of 10^{-4} was omitted).

Table 5

Values ($\times 10^{-4}$) of magnetic parameters for two variants of the 3D BV1 model

Harmonic coefficient	Basic variant			Alternative variant		
	8,25 kA	10,4 kA	Δ	8,25 kA	10,4 kA	Δ
$b(0)_3$	0.622	6.365	−5.743	−0.721	−1.064	0.343
$b(0)_5$	−1.796	0.353	−2.149	−3.529	−3.871	0.342
$b(0)_7$	−1.759	−1.614	−0.145	−2.203	−2.341	0.138
b_3^*	−2.344	6.905	−9.249	−1.06	2.02	−3.08
b_5^*	0.846	2.529	−1.683	−3.783	−4.22	0.437
b_7^*	−2.037	−1.847	−0.19	−4.039	−4.233	0.194

The magnetic parameters for the magnetically active part of BV1, given in Table 5, were calculated for the above-described basic and alternative variants of the cross-section design, optimized at a rated current in the winding.

6. Discussion of results of the 3D calculation of the magnetic characteristics of two variants of the BV1 electromagnet structure

For the convenience of assessing the stability of magnetic parameters when a current changes in the winding from rated to maximal, Table 5 gives the results in three columns for each variant of the structure. In this case, the first column (8.25 kA) gives the calculation results derived at the rated current; the second column (10.4 kA) – at the maximum value of the current. The third column (Δ) gives the difference between the values of the corresponding magnetic characteristics obtained at the maximum and rated current of the winding. The comparison of magnetic characteristics for the two design variants considered, given in the third column in Table 5, indicates a three-fold improvement in the stability of the magnetic parameters in the alternative design. It also follows from the data in Table 5 that a change in the value of a winding power current does not significantly alter the average-integral magnetic induction coefficients b_n^* at $n>3$. This justifies the dominant contribution b_3^* by the third harmonic to the instability of the homogeneity of the transverse magnetic field when the current changes in the winding.

The difference in the values of harmonic coefficients in the central section obtained from a 2D magnetic field model (Tables 2, 4) and based on the 3D calculation (Table 5) is explained by the influence of the following two factors. The first factor is the effect on the end field result created by the ends of the magnetized yoke, which is not accounted for in a 2D model due to the condition for an infinite length of the model of the electromagnet. In addition, the effect of local magnetization created by the transverse elements of winding that are missing from the 2D model has a significant impact. As a result, the value of magnetization at the ends of the yoke is close to saturation. Fig. 14 shows magnetization distributions in cross-section planes for two variants of the electromagnet design (color scales are the same). The two-row variant of the structure has smaller volumes of regions with a magnetization close to the saturation of the yoke material, compared to the base variant.

Another factor directly influencing the value of the minimized average-integral harmonic coefficients is the technological limitations on the accuracy of fabricating the magnetically active part of the BV1 electromagnet. For example, the permissible inaccuracy of laying (geometric position) of winding turns is ±0.05 mm. Therefore, when optimizing the 3D model of the magnetic field and calculating the coefficient b_3^*, the variable size of the structure was changed at a minimum step of 0.1 mm.

This, taking into consideration ratio (10), automatically results in non-zero values of the optimized parameter. However, the proposed technique to slightly alter the length of the winding could be used to correct the value of the average-integral harmonic of magnetic induction in the process of constructing and testing the electromagnet. In order to implement the proposed technique more widely, existing procedures for measuring the magnetic parameters of electromagnets need to be adapted.

7. Conclusions

1. This work has found a magnetic-parameter optimized variant of the structure of a dipole electromagnet with a two-row superconducting winding, which had been used in the construction of the BV1-type electromagnets for the vertical convergence-separation of collider beams at the NICA accelerator complex. The example of the study of the built 2D models for two variants of the structure for the central cross-section of the magnetically active part shows the order of minimization of the coefficients of circular harmonics of the magnetic field in the aperture of the electromagnet. At the same time, the homogeneity of the magnetic field has been investigated as the dependence of non-dipole harmonic coefficients when the current in the superconducting winding changes from 4.0 kA to 10.4 kA.

2. A 3D model of the magnetic field has been created; the calculations of the effective length and average-integral magnetic induction coefficients have been performed on the reference radius of $R_{ref}=0.07$ m for two variants of the structure of the transverse section of the BV1 electromagnet. Based on the analysis of the results of 3D calculations of the magnetic field for the correction of the effective length and the third average-integral harmonic of the magnetic induction in the aperture, ratios were empirically obtained on the basis of the overall dimensions of the electromagnet.

3. The developed variant of the structure with a two-row laying of the winding turns of the dipole electromagnet BV1 demonstrates the minimized contributions to a heterogeneous magnetic field by the average-integral coefficients of harmonics in aperture. In comparison with the classic «window frame» type variant, the alternative version has a reduced value, from $2.344\cdot10^{-4}$ to $1.06\cdot10^{-4}$, of the third average-integral harmonic of the magnetic field. In addition, the alternative option is characterized by a 3-time better (from $\Delta=9.249$ to $\Delta=3.08$) stability of the value of the third harmonic coefficient when the current in the superconducting winding changes.

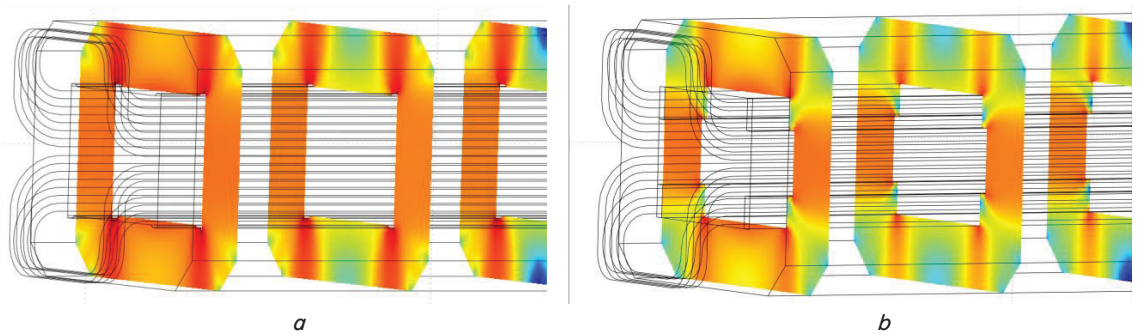

a *b*

Fig. 14. Magnetization distributions in the planes of the cross-section of the electromagnet: *a* – a variant of the «window frame» design; *b* – a variant of the structure with a two-row winding

Referenses

1. Russenschuck, S. (2011). Differential Geometry Applied to Coil-End Design. Field Computation for Accelerator Magnets: Analytical and Numerical Methods for Electromagnetic Design and Optimization. Wiley, 609–636. doi: https://doi.org/10.1002/9783527635467.ch19
2. De Matteis, E., Russenschuck, S., Arpaia, P. (2016). Magnetic field mapper based on rotating coils. CERN-THESIS-2016-147. Available at: https://cds.cern.ch/record/2229576/files/CERN-THESIS-2016-147.pdf
3. Erdelyi, B., Berz, M., Lindemann, M. (2015). Differential Algebra Based Magnetic Field Computations and Accurate Fringe Field Maps. Vestnik SPbGU, 4, 36–55. Available at: https://www.researchgate.net/publication/293654228_Differential_Algebra_Based_Magnetic_Field_Computations_and_Accurate_Fringe_Field_Maps
4. Getman, A. (2018). Cylindrical harmonic analysis of the magnetic field in the aperture of the superconducting winding of an electromagnet. Eastern-European Journal of Enterprise Technologies, 1 (5 (91)), 4–9. doi: https://doi.org/10.15587/1729-4061.2018.123607
5. Tereshonkov, Yu. V., Andrianov, S. N., Jakšić, M., Pastuović, Ž., Tadić, T. (2011). Mathematical modeling of ion microprobes with fringe fields effects. Vestnik S.-Petersburg Univ., 1 (10), 60–75. Available at: http://www.mathnet.ru/links/1d38526c78f98926a424359457b90960/vspui20.pdf
6. Schnizer, P., Fischer, E., Schnizer, B. (2014). Cylindrical circular and elliptical, toroidal circular and elliptical multipoles fields, potentials and their measurement for accelerator magnets. arXiv.org. Available at: https://arxiv.org/pdf/1410.8090.pdf
7. Mierau, A. (2013). Numerische und experimentelle Untersuchungen gekoppelter elektromagnetischer und thermischer Felder in supraleitenden Beschleunigermagneten. Darmstadt. Available at: http://tuprints.ulb.tu-darmstadt.de/id/eprint/3311
8. Trubnikov, G., Sidorin, A., Shurkhno, N. (2014). NICA cooling program. Cybernetics and Physics, 3 (3), 137–146. Available at: http://lib.physcon.ru/file?id=991262ea43a7
9. Khodzhibagiyan, H. G., Agapov, N. N., Akishin, P. G., Blinov, N. A., Borisov, V. V., Bychkov, A. V. et. al. (2014). Superconducting Magnets for the NICA Accelerator Collider Complex. IEEE Transactions on Applied Superconductivity, 24 (3), 1–4. doi: https://doi.org/10.1109/tasc.2013.2285119
10. Getman, A. (2018). Development of the technique for improving the structure of a magnetic field in the aperture of a quadrupole electromagnet with a superconducting winding. Eastern-European Journal of Enterprise Technologies, 5 (5 (95)), 6–12. doi: https://doi.org/10.15587/1729-4061.2018.142163
11. Technical Project of the Object «NICA Complex» (2018). Available at: https://nica.jinr.ru/documents/TDR_spec_Fin0_for_site_eng.pdf
12. Wolff, S. (1992). Superconducting accelerator magnet design. AIP Conference Proceedings, 249. doi: https://doi.org/10.1063/1.41989